This article has been published
In Physica Status Solidi : Rapid Research Letters
https://doi.org/10.1002/pssr.201800590

Article type: Review

Aging in Phase Change Materials : getting Insight from Simulation.

*Jean-Yves Raty**

Dr. J.Y. Raty [1,2]
[1] Physics of Solids, Interfaces and Nanostructures, CESAM group
University of Liège, Allée du 6 Août 19, 4000 Sart-Tilman, Belgium.
[2] CEA-LETI, Université Grenoble Alpes
Minatec Campus, 17 rue des Martyrs, Grenoble, 38054, France

E-mail: jyraty@uliege.be

Keywords: phase change materials, simulation, aging, drift, non-volatile memory

Abstract : Aging is one of the effects limiting the advent of phase change materials as acting components in non-volatile memories. In this paper, we review recent simulation works allowing to describe the underlying microscopic mechanisms that are responsible for the aging of the semiconductor glass and the accompanying resistance drift. In comparison with other systems, the fragile character of Phase Change Materials imposes the use of different methods to sample the space of configurations and the chemical ordering. The emerging picture is that both the evolution of coordination defects and of the underlying network are responsible for the evolution of the electronic properties. The advantage of simulations is that they allow to determine the relation between chemical ordering, the local geometry of atoms and the nature of electronic states. From these correlations, one can extrapolate to obtain the structure of the 'ideal' amorphous state and the relation between bonding in this phase and that of the more conductive crystalline phase. This understanding of microscopic phenomena is crucial to interpret experimental results, but also paves the way to the design of optimized glasses, that are less prone to aging, while preserving the unique properties that place Phase

Change Materials among the best candidates for high performance and scalable non-volatile memories.

1. Introduction

Since their development as data recording materials to be used in non-volatile memories, amorphous Phase Change Materials (a-PCMs) have been shown to exhibit a strong evolution, or drift, of their resistance with time[1] (for a review, see Ref. [2]). This drift is related to the aging phenomenon which is present in all types of glasses, but on timescales that can vary by several orders of magnitudes. In PCMs, that timescale is rather short, and moderate heating can cause an electronic drift to be measurable after a few minutes only (see **Figure 1**).[3] From specific measurements, the electronic drift was attributed to both the enlargement of the band gap with time[4] and to the relaxation gap states.[5-7] This drift of the resistance is a very limiting factor for the development of PCMs in multi-level memories. In these, there is not just one high resistance state, but several of them, that are due to partially crystallized zones within the amorphous phase. With the large drift of the resistance, the recorded data will be modified with time (state 1 would become state 2 etc…). It is therefore not only important to understand the phenomenon, but also to be able to suppress it.

In order to elucidate the role of defects and the global structural evolution during aging and their role in the drift phenomenon, atomistic simulation is the tool of choice. However reproducing the aging of PCMs with simulation is a very challenging task, as we will explain herafter.

First, let us make some general considerations about the physics of glasses (for a review, see Ref. [8]. A glass is a metastable disordered state of matter, which means that upon sufficient energy intake, the glass would crystallize. However, for a given composition, there is not a unique glass configuration, but an extremely large number of structures that are metastable and correspond to local energy minima, as represented in **Figure 2**. With moderate

temperature, the system has an increased probability to jump into a nearby, lower energy minimum.

The local energy minima are structurally connected, and ultimately, at finite temperature, the glass would explore the lowest possible energy minimum that would define the 'ideal' glass. Of course, the overall time for the glass to relax from its initial, rather high energy structure, and reach its ideal configuration, would depend of all the energy barriers encountered along the transition path. This relaxation is called aging, and one directly understands that the process depends on many parameters, starting with the initial structure configuration. Two different mechanisms can be expected to the relaxation of a glass. The first mechanism is the annealing of structural, high energy, coordination defects that are created during the rapid creation of the glass, either by quenching from the melt or from other types of deposition methods such as sputtering in the case of PCMs thin films. The second mechanism involves a more collective rearrangement of the glass structure, and this kind of evolution is usually linked to the decay of the glassy state towards the crystalline one.

2. Aging in glassy Si versus aging in Phase Change Materials

To illustrate these concepts, let us briefly describe one of the most documented family of glasses for which aging is of crucial importance, silicon glasses. In first generation solar cells, the electrical conductivity of hydrogenated amorphous Si (a-HSi) was shown to strongly decrease with time under illumination, but also to recover its initial value afterwards (the Staebler-Wronski effect[9]). In that case, ab initio molecular dynamics (MD) simulations could evidence that overcoordinated Si atoms (fivefold bonded defects) are acting as hole traps, before undergoing a major local structural rearrangement due to the creation of local charges.[10] Therefore, the normal aging of the glass would be explained by the relaxation of these defects back to their initial, neutral state. The role of these defects in the conduction mechanism of a-HSi was explained by ab initio density functional theory (DFT). The

conductivity attributed to variable range hopping at low temperature increases by orders of magnitude at high T due to the strong electron-phonon coupling that is responsible for the delocalization of gap and band tail states.[11] Inversely, one would conclude that the localization of these states would account, at least partially, for the normal aging of an initial high energy glass structure. Vollmayr-Lee et al. have indirectly simulated aging in a-Si[12] with classical potentials by varying the cooling rate and attributed the aging to variations in the angles inside and between units of the tetrahedral network, later confirmed by tight binding simulations.[13] In those cases, aging is thus more related to a global evolution of the structure towards the crystal local order rather than to an evolution of defects.

Which of these mechanisms applies to a-PCMs, given the fact that there are fundamental differences between a-Si and a-PCM? First, silicon is a strong glass former, while PCMs are poor glass formers, thus prone to recrystallization, and have a high fragility index. This high fragility implies that the synthesis, often performed by quenching from the melt (MQ), has to be extremely rapid. The amorphous phase thus 'freezes' on a very short time and within a small temperature range (see for example [8, 14]), it is thus locked in a very high energy initial metastable state. For amorphous silicon, it is not the case, since its structure is essentially similar to that of the crystal, with angular fluctuations between sp3 bonded atoms, these fluctuation decreasing with aging,[12] the glass behaving as in the classical Zachariasen picture. [15] This structural analogy between amorphous and crystal does clearly not hold for PCMs, as evidenced by many experiments (diffraction, EXAFS…[2]). For PCMs, aging appears to be more complex as both the type of bonding and local high energy defects are suspected to evolve with time. Besides the drift effect, aging in thin film PCMs is accompanied by a release of stress (the amorphous volume contracts),[16] which suggests large atomic rearrangements.

Experimentally, the drift phenomenon has been evidenced in all PCMs, with compositions as different as GeTe, $Ge_xSb_yTe_z$ (GST), Sb_2Te_3, or $Ag_4In_3Sb_{67}Te_{26}$ (AIST)[17]. The strong

evolution of the resistance with time has been observed not only in deposited thin films [3, 5] but also in actual memory cells [6, 18]. Modulated photocurrent and photothermal deflection spectroscopy measurements allowed to measure similar defects states in GeTe and $Ge_2Sb_2Te_5$, which are located about 0.2 and 0.5 eV above the top of the valence band [5]. If the evolution of these states' distributions with aging is unclear, a pronounced increased of the band gap was observed, which was also evidenced upon annealing of the AIST PCM [17]. From these measurements several models have been proposed. Ielmini and coworkers have explained the drift by structural relaxation,[19] whereas Luckas et al. have measured the low activation energy for conduction, in correlation with the drift coefficient.[20] Often, the transport properties have been modelled with a hopping between trap states process, the distance between the traps and their occupation varying with time and temperature. [7] To understand these measurements it is necessary to disentangle the role of 'defects' and of the global amorphous structure onto the electronic density of states and its localization features. Experimentally, a few experiments have been performed to measure the evolution of some PCMs' structure upon aging in [21, 22] using X-ray absorption. The EXAFS spectrum of GeTe indicated the increase of the proportion of short Ge-Ge bonds upon aging, possibly explained either by the creation of tetrahedral Ge units, or by some segregation of Ge atoms, whereas in $Ge_2Sb_2Te_5$, on the contrary, the evolution of the XANES spectrum with aging was explained by a progressive disappearance of Ge tetrahedral environments.

3. Simulation of amorphous PCM : structure and defects.

Simulation is clearly a tool that could help to disentangle these effects and to elucidate the driving mechanism for the aging of a-PCM. In this specific case, ab initio-based tools are required since one needs a high quality representation of the electronic structure, to study the drift effect, and the transferability of the methods to very different environments, which

mostly prevents the use of semi-empirical schemes. This approach has been developed by many groups in the last fifteen years, [23-36] [37-50] though the technical details of the ab initio density functional theory (DFT) simulations differ widely among studies, as do the analyses and interpretation of the results.

In order to understand aging, one first has to know the structure of the initial amorphous phase, to describe the coordination defects and have a description of the electronic structures (gap, defect states, localization properties…). The most usual method adopted to generate an amorphous structure is the quench from the melt, which in the simulations corresponds to cooling the liquid down to ambient temperature with a typical gradient of 5-20K per picoseconds, thus orders of magnitude faster than in experimental quenching. Another approach, that simulates a sputter deposition process, was used in Ref.[32]. In that study, atoms are sent in a random fashion towards the surface of a GST225 slab, with controlled temperature. The models obtained ausing ab initio MD are very similar in terms of coordination numbers, proportion of species etc… despite the use of different exchange-correlation functionals (i.e. PBE, PBEsol[51], BLYP[42, 44, 46], TPSS[26]) and the treatment, or absence thereof, van der Waals interactions, either with a self-consistent treatment of the electrons (vdw-DF2[45, 52]) or in a semiempirical fashion (Grimme D2 [44, 47][53]).

The resulting structures for Ge-based amorphous PCMs are generally discussed in terms of tetrahedral motifs and distorted octahedra (see **Figure 3**). The relative proportions of 3-fold, 4-fold (tetrahedral or with right angles, labeled as see-saw in Figure 2) and 5-fold bonded Ge atoms vary with the study, however this already suggests that different Ge bonding environments (which relate to different bonding types, from sp3 to p-bonding) are of comparable energies. Therefore, one can already guess that many glass configurations are competing during relaxation and aging.

Among all studies, the works by Akola et al.[32] and Bouzid et al.[46] provide models for amorphous Ge2Sb2Te5 (GST225) that vary significantly from all other works. In Ref.[32] a

much larger proportion of tetrahedrally bonded Ge atoms (71% after optimization at 0K) is found in the model created by simulating the sputter deposition process in comparison with the model obtained by MQ (42%). This difference was attributed to a larger proportion of Ge-Ge bonds in the deposited sample and to the fact that simulated MQ allows for more chemical homogeneity in the system. The MQ model is lower in energy and has a larger gap which indicates that the deposited sample is more out-of-equilibrium and more distant to an 'ideal' amorphous structure. By extrapolation of these results, aging could possibly be related to the disappearance of tetrahedral Ge. However, tetrahedral Ge atoms are not the only species responsible for a smaller gap, as shown in **Figure 4**. For instance, two-fold bonded Te atoms are also contributing to localized states in band tails.[42] The work by Bouzid et al.[46] is singular as it obtains 69% of tetrahedral Ge atoms, with 9% of Ge-Ge bonds, but for a MQ model, that appears to be in reasonable agreement with the experimental data. The electronic structure is analysis claimed the presence of lone pairs on both Te atoms and non-tetrahedral Ge atoms. In a study of amorphous GeTe,[44] it was shown that the inclusion of the Grimme correction to account for van der Waals forces is producing 81% of tetrahedral Ge atoms (together with 57% of twofold bonded Te atoms), correlated with numerous (45%) and extremely short Ge-Ge distances (most of them shorter than 2.5Å). That model provides an improved agreement with the experimental structure factor in comparison with standard DFT calculations with PBE, in which 28% of Ge atoms are tetrahedrally bonded but still counts 39% of Ge-Ge bonds. To our knowledge, these results differ from all other MQ a-GeTe models, including those obtained with an ab initio treatment of dispersion forces.[52]

Totally independent on the way amorphous GeTe and GST models are produced, it appears clearly that those models with more tetrahedral Ge are closer agreement with the experimental structural data (diffraction, EXAFS). In view of Akola's work,[32] this seems reasonable, knowing that the mentioned experiments are performed on sputter-deposited samples, while most simulations deal with MQ models. These MQ models would rather correspond to the

amorphous structure inside a memory cell and obtained by Joule heating and subsequent fast quenching of a PCM crystal.

4. Simulating Aging in PCM

4.1 Limitations of Molecular Dynamics

Having a description of the initial state for an amorphous PCM is not sufficient to understand aging and the related drift of the electronic properties. One has to answer other questions. What is the 'ideal' amorphous structure, or amorphous structure with the lowest possible energy, knowing that it has to be metastable enough (sufficient energy barrier to crystallization) to avoid crystallization? What is the pathway between the initial amorphous and this ideal case? What are the associated energy differences (basically, one would like to be able to draw the potential energy landscape as schematized in Figure 1)?

Answering these questions is a very challenging task that is clearly not achievable with regular ab initio molecular dynamics due to the total mismatch between the timescale for simulations (at best a few nanoseconds) and the experimental times, that is measured at least in minutes (if accelerated by moderate temperature annealing). Actually, due to the high fragility index of PCM, the only full ab initio molecular dynamics studies performed at finite temperature were intended to study the crystallization process. However, a strong evolution of the amorphous structure towards that of the crystal was observed (at 600K) by Loke and coworkers[35] who use this modification of the amorphous structure to speed up the crystallization process. The pre-structuring consists of an increase in the number of square patterns (connected octahedral entities) with the right alternating chemical order. A similar observation was reported by Kalikka and coworkers,[51] who also emphasize the concomitant decrease in the number of tetrahedral Ge atoms. However, one cannot simply extrapolate that the rearrangements occurring in the amorphous at high temperature (600K) are the same as

those that happen on a timescale that differs by several orders of magnitude at moderate (including ambient) temperature.

4.2 Simulation using chemical substitution

Instead of the direct molecular dynamics approach, one has to resort to using alternative methods to sample the space of configurations for the a-PCM and obtain a description of the potential energy landscape. One of the approaches consists of generating amorphous models of various structures and energies (having sometimes very high values), before relaxing them and analyzing their properties. This is what was performed in Ref.[52] where amorphous structures were generated for several chalcogenides compositions (SiTe, GeSe, SnTe) before substituting species to obtain the right GeTe composition, and comparing with regular MQ GeTe models. The initial models differed widely and needed to be annealed with the GeTe composition to reach reasonable energy values. The large number of structures allowed to evidence statistical correlations between the chemical order (measured by the number of homopolar Ge-Ge bonds), the number of tetrahedral Ge atoms, the stress, and the energy of the system. Indeed, the energy of the models decreases with the decrease of the number of homopolar bonds and of the proportion of tetrahedral Ge atoms, as observed in Ref.[32]. At the same time, the stress is reduced inside of the simulation box. It should be noted that the different models are uncorrelated and therefore no direct interpretation can be drawn about the structural relaxation pathway of the amorphous and its dynamics. The models would rather correspond to some instantaneous snapshots observed along a Monte Carlo simulated annealing trajectory.

Using a chemical potential approach, it was possible to extract the dependence of the local energy of atoms as a function of their local order (see **Figure 5**). It could be observed that for Ge atoms, both the tetrahedral environment and a 3-fold crystal-like environment have a low energy, whereas the defective octahedron with 4 neighbors bonded at right angles appear as

some transition state between both minima. Interestingly, one should not limit the analysis to Ge atoms (the stress would increase), but also consider the combined evolution of Te atoms. For these, a single minimum is observed for 3-fold bonded atoms, the creation of which being responsible for the overall decrease in stress. It is interesting to note that tetrahedral Ge atoms have a both a low energy and small volume. A simple calculation could then show that the fact that they include at least one homopolar Ge-Ge bond imposes the existence of two-fold bonded Te atoms in the structure. These have energies slightly above those of three-fold bonded Te atoms and occupy a much larger volume, and would thus ctreate some stress. However, one can not totally neglect the possibility, especially since entropy is neglected in this study, that although SnTe-like amorphous GeTe structures appear to be closer ideality, the relaxation of the glass from a high energy state (with many Ge-Ge and Ge^{H} geometries, see Figure 5), could produce a different kind of topology, dominated by tetrahedral Ge units and 2-fold Te atoms.

In summary, by comparing the energetics of all local geometries in all models, it was possible to explain aging by the transformation of a structure in which a majority of the Ge atoms are tetrahedrally coordinated (with at least one Ge neighbor) mixed with Te atoms that are predominantly two-fold bonded, to a structure in which the dominating species are 3-fold Ge atoms bonded with 3-fold bonded Te atoms. A deeper analysis of these species showed that they result from large local, Peierls-like, distortions of octahedral environments, the distortion increasing with aging. Interestingly, this last relaxation could also account for aging in Ge-free glasses such as Sb2Te3 or AIST. This is quite similar to the picture drawn by Huang et al.[31] in which an amorphous PCM structure was compared to a crystal structure with very large distortions (mostly angular). In Ref.[43], it was observed that the proposed relaxation of amorphous GeTe resulted in an opening of the DOS gap, together with a strong localization of residual gap states.

4.3 Simulation using metadynamics

A possible limitation of the models proposed in Ref.[43] is that, though a rather large number of independent structures are analyzed to propose a model for aging, the size of the simulating box was limited, which prevents the accurate reproduction of an extended range order. A possible way to bypass this limitation is to adjust a potential or forcefield to reproduce some reference structures and then to apply these for simulations on larger boxes. This is what was done by Sosso and coworkers[48] who developed a numerical neural-network (NN) potential that was trained to reproduce the forces and total energies of a very large number (about 30000) of ab initio GeTe structures. Indeed, such a large database of crystalline and disordered (realistic or less realistic) structures was required so as to reproduce the ab initio structure of liquid and amorphous GeTe and obtain predictive power. The main discrepancy between ab initio and neural network MQ amorphous structure resides in the slightly larger number of Ge-Ge bonds in the latter, however the final amorphous structure for a 4096 atoms model quenched from the liquid in 100ps is very similar to the structure generated using ab initio MD simulations, with a majority of 4-fold bonded Ge and 3-fold bonded Te atoms. Most Ge atoms adopt a defective octahedral coordination with angles close to 90 and 180° (labeled as Ge_H in Figure 4), but about 20-30% of them have a tetrahedral coordination. and. The NN potential, complemented by a Grimme D2 correction to account for van der Waals forces, was also able to measure the deviation from the Stokes-Einstein relation in undercooled GeTe[36] by extending the simulations trajectories up to 2 ns. If the NN potential allows to overcome the problem of the size of the system, it was necessary for the authors to sample the configurational space by a different method from molecular dynamics in order to simulate aging, namely metadynamics (see **Figure 6**).

In this method, the potential energy landscape of the amorphous system is explored by adding energy penalties for each configuration sampled along the dynamics trajectory. The added

penalty potential is chosen as a gaussian function of some collective coordinates that depend on the ions positions. In that case, the variables describing an instantaneous structure are the number of Ge-Te and Ge-Ge bonds in presence of Ge chains. This ensures that Ge-Ge chains would disrupt as the metadynamics is going on (see **Figure 7**), allowing the system to explore other energy basins. Despite the use of a totally different approach, similar observations to those in Ref.[52] were made. The removal of Ge-Ge bonds leads to lower energy structures, with slightly lower proportion of tetrahedral Ge (-3%), and to the enlargement of the gap from 0.21eV to 0.23eV. The same potential was used[54] to simulate the crystallization and aging of a GeTe nanowire. The structure of the wire indicates a different composition at the surface than in bulk GeTe, with 72% Te and 28% Ge, about half of which being tetrahedrally bonded. The length of Ge-Ge chains, indicative of Ge atoms clustering, inside the wire appears to be smaller than in the bulk, which removes most of the gap states. Though no actual simulation of aging was performed, the authors interpreted their result as a sign that the removal of Ge-Ge chains (and the often associated tetrahedral Ge) leads to lower energy amorphous structure, with fewer defect states.

Recently, a similar neural network potential was developed for the ternary compound Ge2Sb2Te5 by Mocanu and coworkers[49] and it was applied to simulate the structure of an amorphous system with 7200 atoms. The neural network was shown to reproduce quite well the structure factor obtained from a regular DFT simulation on a ‘small’ system (315 atoms), yet, this potential yields a much lower proportion of tetrahedral species (down to 5%). Simulating the evolution of this initial large MQ structure during aging (for instance with a metadynamics study) is still to be performed.

4.4 Simulation using a Metropolis algorithm

The last simulation study of drift was performed by Zipoli and coworkers[55], following a quite different, and original, approach. First, they simulate a number of amorphous GeTe using classical molecular dynamics. The potential used is a modified Tersoff potential, which allows to produce a large number of trajectories (on 216 atoms cells) simulating the quenching from the liquid phase to 300K in 4 nanoseconds. As one cannot expect such a potential to approach the quality of ab initio results, the authors relaxed their final structures with regular DFT. As said before, such MD trajectories do not allow for sufficient sampling of the configurational space, and yield structures with a chemical order that bear strong resemblances with the initial liquid (see Ref.[52]). To obtain structures that sample the chemical order and obtain a statistical description of the amorphous potential energy landscape, a modified potential was used in which the attraction term between Ge atoms and that between Te atoms was set to zero. This created structures with the strongest alternation of species. The authors also generated a number of trajectories in which random pairs of Ge and Te atoms were switched using a Metropolis algorithm (replica exchange method). All those amorphous structures were then used to compute the optical conductivity (with a hybrid functional), and a correlation between local topology and conductivity was determined (see **Figure 8**).

From this analysis, it was concluded that the 'ideal' amorphous, being defined in that work as that having the largest resistance, was an amorphous with fewer 4-fold (tetrahedral and defective octahedral order) Ge and more 3-fold bonded Ge, and in which the Ge-Te alternation is maximal. This gives further support to the picture from the two studies we described before[52, 56], however Zipoli and coworkers attribute the change in conductivity to the removal of gap states more than to the opening of the gap, which does not seem to account for some recent experimental developments[4].

So, in summary, all studies (note that these have been performed on GeTe only) yield the same picture indicating that the aging and the related drift of the glass is due to the

progressive breaking of Ge-Ge bonds, which destabilizes tetrahedral and other 4-fold bonded species in favor of 3-fold bonded Ge atoms. These were shown in Ref.[52] to be octahedra with a very strong local distortion that creates three very short distances (quite shorter than in the crystal) and three other distances that are much longer than in the crystal. At the same time, Te atoms evolve from being mainly two-fold bonded to being three-fold bonded. If the aged amorphous structure clearly reminds features from the crystalline structure (that results from a more moderate Peierls distortion of a face centered cubic structure[57]), with a pronounced p-bonding character, it moves away from the crystal local order with further relaxation. In that sense, it does not match the classical Zachariasen glass picture[15]. As we have seen, simulation can give a detailed description of the aging process, but does it agree with the available structural measurements? This remains arguable, as some interpretation of XANES measurements of amorphous Ge2Sb2Te5 led to the conclusion that the number of tetrahedrally bonded Ge atoms is indeed decreasing with aging, while another study by Noé et al.[21] on GeTe yielded exactly the inverse conclusion from the analysis of the XANES spectra. One of the possible reason for this discrepancy could eventually be found in the inhomogeneities that are inherent to the sputter deposition process, and that are very unlikely to be observed in the simulated high temperature liquid that is precursor to the amorphous in a MQ simulation, but also during a metadynamics simulation as in Ref.[56] or in a mixed Molecular Dynamics - Monte Carlo-like simulation as in Ref.[55].

5. Limiting aging : adjusting mechanical constraints.

Now, one can wonder whether these information gathered from simulation can help designing amorphous phase change materials that are less prone to aging. First, the homogeneity of the deposition in the sputtering process is an important parameter that could prevent having an initial amorphous state that would include a large proportion of tetrahedral Ge atoms (favored when Ge-Ge bonds are formed). It is also clear that limiting electromigration inside a memory

cell would decrease the importance of aging, and thus of the resistance drift. Second, one could think of stabilizing the amorphous by including elements that will modify the glass network topology as proposed in Ref.[38]

This could be inferred from **Figure 9**, in which a clear correlation is established between the energy of the GeTe glass and the number of topological constraints[58]. The number of such constraints can be computed for a glassy atomic network by counting the number of rigid bonds (that have a small associated Debye-Waller factor) and the number of rigid angles (that have a small angular excursion upon vibration) around each individual atom[29]. It appears that the transformation of the network from being composed mainly of 4-fold bonded Ge atoms and 2-folded bonded Te atoms into a network consisting mostly of 3-fold bonded Ge and Te atoms decreases the number of mechanical constraints at the microscopic level.

Actually the decrease of such mechanical constraints was shown to increase the density of low frequency vibrational modes (Boson peak[59]) in stressed-rigid glasses such as GeTe[29]. On the other hand this increase of the Boson peak's height has been associated with larger mean squares displacements[60], that could facilitate overcoming local potential energy barriers, and help the structural evolution of the glass. If the direct connection between rigidity, through the number of mechanical constraints, and aging has not been demonstrated, a correlation was established in the case of carbon and nitrogen-doped GeTe[38] between the number of constraints, the density of low frequency vibrational modes and a higher activation energy for crystallization, meaning a more stable amorphous structure.

6. Concluding remarks.

Understanding the aging and the drift of Phase Change Materials using simulation is not an easy task and requires to overcome a number of difficulties. First, one has to obtain a reliable structure of the amorphous structure, which in the case of PCM is already a delicate matter. Indeed, the high fragility index is such that the glass structure obtained by the melt-and-

quench technique has a chemical order that resembles that of the liquid, and the annealing of coordination defects is a very slow process. Second, several types of Ge atoms geometries are of comparable energy and therefore the structure is not as simple to interpret as that of Zachariasen glasses such as silicon glasses. Indeed, the 8-N rule that is not verified in crystalline PCM (GeTe or metastable cubic GST), is also not verified, on average, in the initial glass structure as well. Third, the relaxation occurring during aging involves breaking bonds and rearranging the structure, which is an extremely slow process. Therefore, some simulation tricks have to be used in order to better sample the space of configurations of the amorphous system and find the relaxation pathway towards an 'ideal' amorphous structure. As for now, three different approaches have been adopted, all of them applied to the archetypal GeTe case, that use either chemical substitution, metadynamics or Monte-Carlo like permutations of atoms. Sometimes, numerical or classical potentials have been used to produce structures on longer time scales or with more atoms, before analyzing the results ab initio to study the modification of the electronic structure. These works have led to remarkably similar pictures of aging. Homopolar Ge-Ge bonds that are already present in the liquid structure, and even more numerous in the sputter-deposited samples, favor a large proportion of tetrahedral Ge environments and sp3 bonding, together with 2-fold bonded Te, thus matching the 8-N rule for both species. However, these motifs create smaller gaps and numerous localized gap states. The relaxation of the glass breaks the Ge-Ge bonds, favoring 3-fold Ge and Te atoms and p-bonding type. Though this coordination is the same as in the stable GeTe crystal, further relaxation increases the local Peierls distortion (and angular fluctuations), which stabilizes the amorphous against crystallization. On the contrary, heating the amorphous structure reduces the amplitude of the Peierls distortion, which was shown to be an efficient way to incubate crystallization[35]. It is possible that the increase of the Peierls distortion upon relaxation could account for aging in Ge-free compounds such as Sb2Te3 and AIST, and would then appear as a common relaxation mechanism for PCMs, but this has to

be confirmed by specific simulation studies. Finally, ab initio simulations could be used to help finding new compositions, around that of known PCMs, that would be less prone to aging thanks to the minimization of the number of mechanical constraints.

Acknowledgements

J.-Y.R. acknowledges computational resources provided by the CÉCI funded by the F.R.S.-FNRS under Grant No. 2.5020.11 and the Tier-1 supercomputer of the Fédération Wallonie-Bruxelles, infrastructure funded by the Walloon Region under grant agreement n°1117545. J.-Y.R acknowledges support from the Communaute Française de Belgique through an ARC grant (AIMED 15/19-09).

Received: ((will be filled in by the editorial staff))
Revised: ((will be filled in by the editorial staff))
Published online: ((will be filled in by the editorial staff))

References

[1] A. Pirovano, A. L. Lacaita, F. Pellizzer, S. A. Kostylev, A. Benvenuti, R. Bez, *IEEE Trans. Electron Devices* **2004**, *51*, 714.

[2] P. Noé, C. Vallée, F. Hippert, F. Fillot, J.-Y. Raty, *Semicond. Sci. Tech.* **2017**, *33*, 013002.

[3] D. Krebs, R. M. Schmidt, J. Klomfaβ, J. Luckas, G. Bruns, C. Schlockermann, M. Salinga, R. Carius, M. Wuttig, *J. Non·Cryst. Solids* **2012**, *358*, 2412.

[4] M. Rütten, M. Kaes, A. Albert, M. Wuttig, M. Salinga, *Sci. Rep.* **2015**, *5*, 17362.

[5] J. Luckas, D. Krebs, S. Grothe, J. Klomfaß, R. Carius, C. Longeaud, M. Wuttig, *J. Mater. Res.* **2013**, *28*, 1139.

[6] M. Boniardi, D. Ielmini, *Appl. Phys. Lett.* **2011**, *98*, 243506.

[7] M. Kaes, M. Salinga, *Sci. Rep.* **2016**, *6*, 31699.

[8] J.-Y. Cho, T.-Y. Yang, Y.-J. Park, Y.-C. Joo, *Electrochem. Solid St.* **2012**, *15*, H81.

[9] C. A. Angell, K. L. Ngai, G. B. McKenna, P. F. McMillan, S. W. Martin, *J. Appl. Phys.* **2000**, *88*, 3113.

[10] D. Staebler, C. Wronski, *Appl. Phys. Lett.* **1977**, *31*, 292.

[11] E. Johlin, L. K. Wagner, T. Buonassisi, J. C. Grossman, *Phys. Rev. Lett.* **2013**, *110*, 146805.

[12] T. Abtew, M. Zhang, D. Drabold, *Phys. Rev. B* **2007**, *76*, 045212.

[13] K. Vollmayr, W. Kob, K. Binder, *Phys. Rev. B* **1996**, *54*, 15808.

[14] N. Bernstein, J. Feldman, M. Fornari, *Phys. Rev. B* **2006**, *74*, 205202.

[15] W. H. Zachariasen, *J. Am. Chem. Soc.* **1932**, *54*, 3841.

[16] S. Caravati, M. Bernasconi, T. D. Kühne, M. Krack, M. Parrinello, *Appl. Phys. Lett.* **2007**, *91*, 171906.

[17] W. Wełnic, S. Botti, L. Reining, M. Wuttig, *Phys. Rev. Lett.* **2007**, *98*, 236403.

[18] J. Akola, R. O. Jones, *Phys. Rev. Lett.* **2008**, *100*, 205502.

[19] J. Akola, R. O. Jones, S. Kohara, S. Kimura, K. Kobayashi, M. Takata, T. Matsunaga, R. Kojima, N. Yamada, *Phys. Rev. B* **2009**, *80*, 020201.

[20] J. Hegedus, S. Elliott, *Phys. Status Solidi A* **2010**, *207*, 510.

[21] J.-Y. Raty, C. Otjacques, J.-P. Gaspard, C. Bichara, *Solid State Sci.* **2010**, *12*, 193.

[22] M. Micoulaut, J.-Y. Raty, C. Otjacques, C. Bichara, *Phys. Rev. B* **2010**, *81*, 174206.

[23] R. Mazzarello, S. Caravati, S. Angioletti-Uberti, M. Bernasconi, M. Parrinello, *Phys. Rev. Lett.* **2010**, *104*, 085503.

[24] B. Huang, J. Robertson, *Phys. Rev. B* **2010**, *81*, 081204.

[25] J. Akola, J. Larrucea, R. Jones, *Phys. Rev. B* **2011**, *83*, 094113.

[26] G. Ghezzi, J.-Y. Raty, S. Maitrejean, A. Roule, E. Elkaim, F. Hippert, *Appl. Phys. Lett.* **2011**, *99*, 151906.

[27] J. Kalikka, J. Akola, J. Larrucea, R. Jones, *Phys. Rev. B* **2012**, *86,* 144113.

[28] D. Loke, T. Lee, W. Wang, L. Shi, R. Zhao, Y. Yeo, T. Chong, S. Elliott, *Science* **2012**, *336,* 1566.

[29] G. C. Sosso, J. Behler, M. Bernasconi, *Phys. Status Solidi B* **2012**, *249,* 1880.

[30] S. J. Park, M. H. Jang, S. J. Park, M. Ahn, D. B. Park, D.-H. Ko, M.-H. Cho, *J. Mater. Chem.* **2012**, *22,* 16527.

[31] J.-Y. Raty, P. Noé, G. Ghezzi, S. Maîtrejean, C. Bichara, F. Hippert, *Phys. Rev. B* **2013**, *88,* 014203.

[32] B. Prasai, M. E. Kordesch, D. A. Drabold, G. Chen, *Phys. Status Solidi B* **2013**, *250,* 1785.

[33] W. Zhang, I. Ronneberger, P. Zalden, M. Xu, M. Salinga, M. Wuttig, R. Mazzarello, *Sci. Rep.* **2014**, *4,* 6529.

[34] V. L. Deringer, W. Zhang, M. Lumeij, S. Maintz, M. Wuttig, R. Mazzarello, R. Dronskowski, *Angew. Chem. Int. Edit.* **2014**, *53,* 10817.

[35] S. Caravati, M. Bernasconi, *Phys. Status Solidi B* **2015**, *252,* 260.

[36] J.-Y. Raty, C. Otjacques, R. Peköz, V. Lordi, C. Bichara, in *Molecular Dynamics Simulations of Disordered Materials: From Network Glasses to Phase-Change Memory Alloys* (Eds: C. Massobrio, J. Du, M. Bernasconi and P. S. Salmon), Springer, Cham, Switzerland, **2015**, pp. 485-509.

[37] M. Micoulaut, A. Piarristeguy, H. Flores-Ruiz, A. Pradel, *Phys. Rev. B* **2017**, *96,* 184204.

[38] H. Weber, M. Schumacher, P. Jóvári, Y. Tsuchiya, W. Skrotzki, R. Mazzarello, I. Kaban, *Phys. Rev. B* **2017**, *96,* 054204.

[39] A. Bouzid, G. Ori, M. Boero, E. Lampin, C. Massobrio, *Phys. Rev. B* **2017**, *96,* 224204.

[40] A. Bouzid, C. Massobrio, M. Boero, G. Ori, K. Sykina, E. Furet, *Phys. Rev. B* **2015**, *92,* 134208.

[41] G. C. Sosso, G. Miceli, S. Caravati, J. Behler, M. Bernasconi, *Phys. Rev. B* **2012**, *85*, 174103.

[42] F. C. Mocanu, K. Konstantinou, T. H. Lee, N. Bernstein, V. L. Deringer, G. Csányi, S. R. Elliott, *J. Phys. Chem. B* **2018**,

[43] C. Qiao, Y. Guo, F. Dong, J. Wang, H. Shen, S. Wang, M. Xu, X. Miao, Y. Zheng, R. Zhang, *J. Mater. Chem. C* **2018**, *6*, 5001.

[44] J. Kalikka, J. Akola, R. O. Jones, *Phys. Rev. B* **2014**, *90*, 184109.

[45] J. Y. Raty, W. Zhang, J. Luckas, C. Chen, R. Mazzarello, C. Bichara, M. Wuttig, *Nat. Commun.* **2015**, *6*, 7467.

[46] the semi-empirical nature of the Grimme D2 functional is arguable as the functional dependency on the local atomic environment is fixed and the internal polarizabilty coefficients are not adjusted to experimental values but to ab initio computed reference values instead.

[47] S. Gabardi, E. Baldi, E. Bosoni, D. Campi, S. Caravati, G. Sosso, J. Behler, M. Bernasconi, *J. Phys. Chem C* **2017**, *121*, 23827.

[48] F. Zipoli, D. Krebs, A. Curioni, *Phys. Rev. B* **2016**, *93*, 115201.

[49] S. Gabardi, S. Caravati, G. Sosso, J. Behler, M. Bernasconi, *Phys. Rev. B* **2015**, *92*, 054201.

[50] J. Gaspard, F. Marinelli, A. Pellegatti, *EPL* **1987**, *3*, 1095.

[51] P. Noé, C. Sabbione, N. Castellani, G. Veux, G. Navarro, V. Sousa, F. Hippert, F. d'Acapito, *J. Phys. D: Appl. Phys.* **2015**, *49*, 035305.

[52] A. Piarristeguy, A. Pradel, J.-Y. Raty, *MRS Bulletin* **2017**, *42*, 45.

[53] H. M. Flores-Ruiz, G. G. Naumis, *Phys. Rev. B* **2011**, *83*, 184204.

[54] H. M. Flores-Ruiz, G. G. Naumis, *J. Chem. Phys.* **2009**, *131*, 154501.

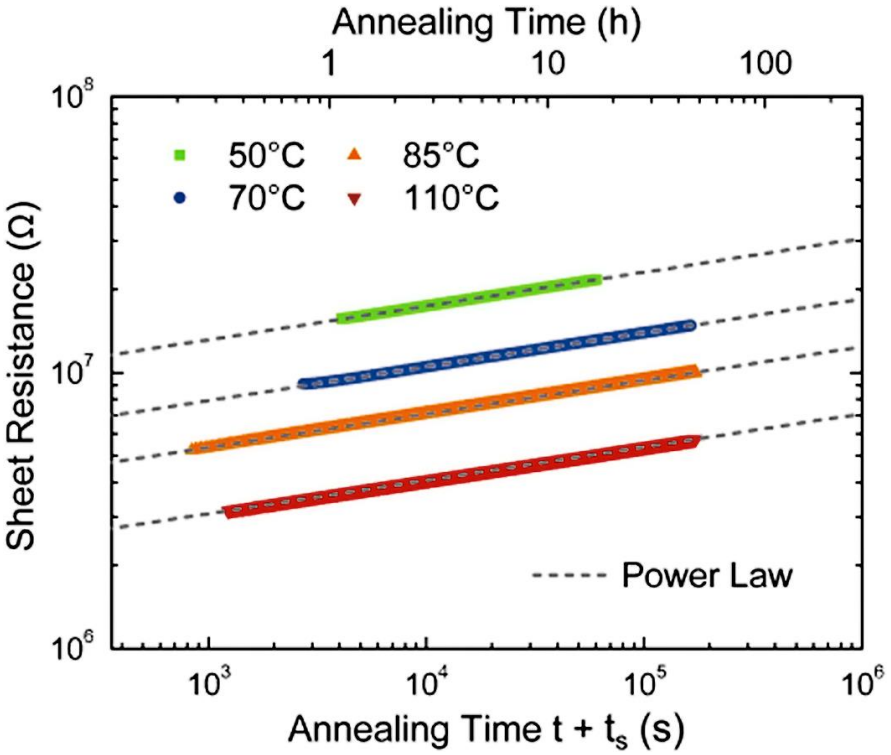

Figure 1. Evolution of the electrical resistance in thin film GeTe annealed at various temperatures. The increase of resistance, or drift, follows a power law with a slope that is independent of the temperature of annealing. The drift is linked to the aging of the glass, that is accelerated by temperature. Reproduced with permission.[3] Copyright 2012, Elsevier.

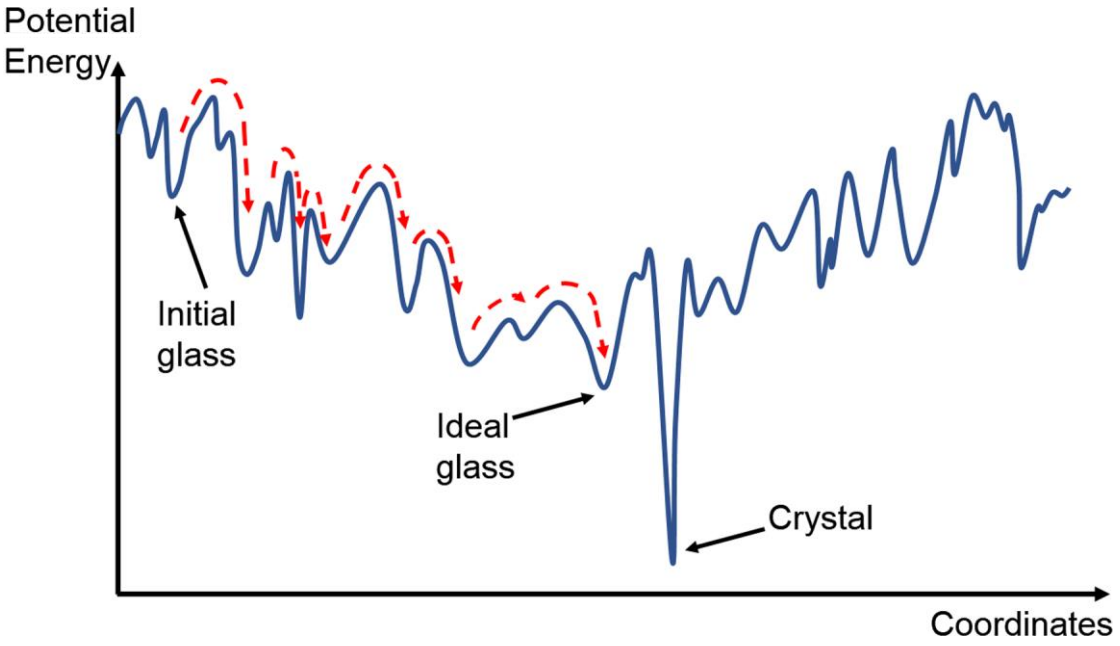

Figure 2. Schematic energy landscape for a glass, for which hopping (indicated by the dashed arrows) can proceed between many local energy minima separated by small energy barriers. The 'ideal' glass is the global minimum, keeping in mind that the glass is metastable and that the system can evade from this global minimum by overcoming a larger activation barrier, in that case to crystallization. Figure inspired from the review of Angell et al.[8].

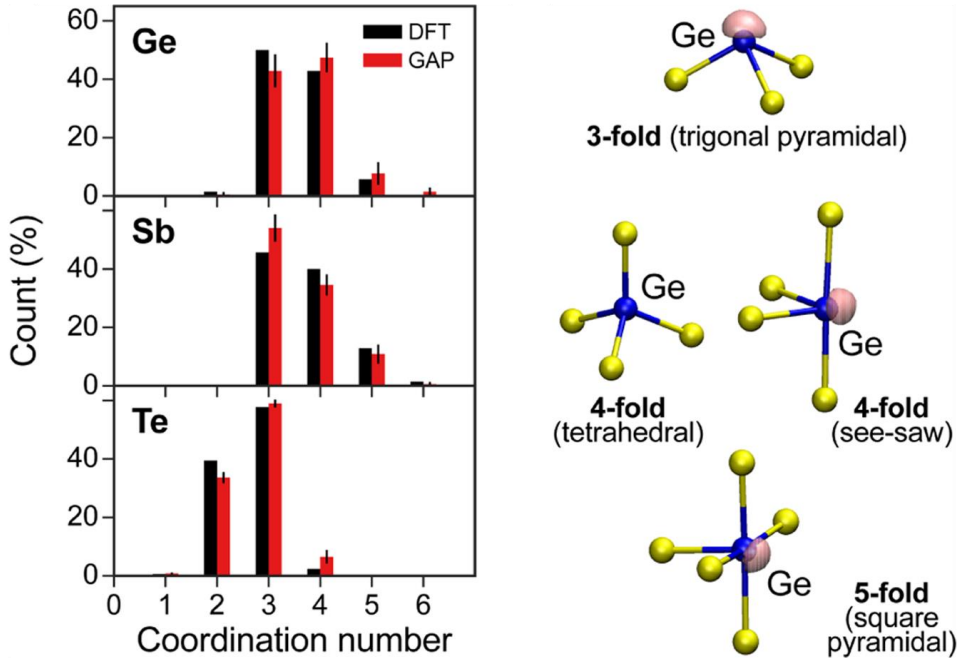

Figure 3. Coordination number distribution in amorphous GST225 simulated using pure DFT and with a neural network potential (GAP).[49] The local atomic arrangements around Ge atoms found in the structure are shown on the right. The isosurface (drawn at 0.85-0.9 value) of the ELF (electron localization function) is shown in purple, indicating zones containing electrons with a high kinetic energy, thus more localized (note that this representation does not give any indication about the density of electrons, which can eventually be very low, in these pockets). Reproduced with permission.[49] Copyright 2018, American Chemical Society.

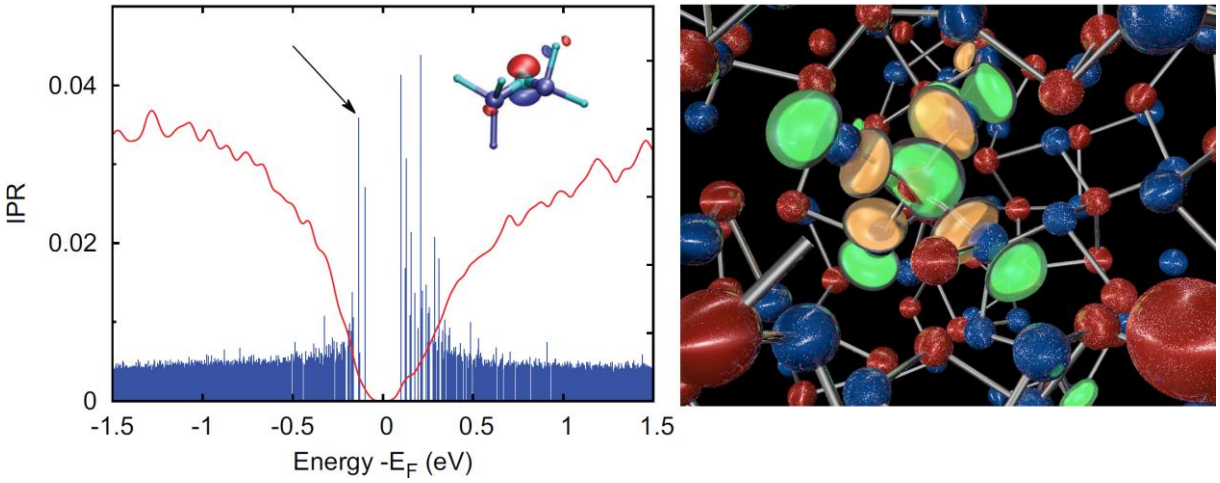

Figure 4 : (Left) Density and localization of states, as measured by the Inverse Participation Ratio, of amorphous Ge2Sb2Te5 obtained by the melt-and-quench approach.[42] The density of states in red is superposed to the Inverse Participation ratio values, in blue, for all eigenstates. The inverse participation is computed for each electronic state by effectively measuring a number of atomic orbital projections, with normalizing. A value of 1 would mean perfect localization, a value of 1/N, N being the total number of possible atomic orbitals projections in the simulation box, would mean perfect delocalization. The figure shows the increased localization of band tail states. One of the most localized states (indicated by the arrow) is represented in the inset, showing a major contribution of a lone pair on a 2-fold bonded Te atom. Reproduced with Permission.[42] Copyright 2017, John Wiley and Sons.

(Right) Example of a mid-gap state defect (localized with IPR=0.44) in relaxed amorphous GeTe.[52] The state is fully localized on a tetrahedral Ge atom bonded to four 2-fold bonded Te atoms (Ge atoms are in red, Te atoms in blue).

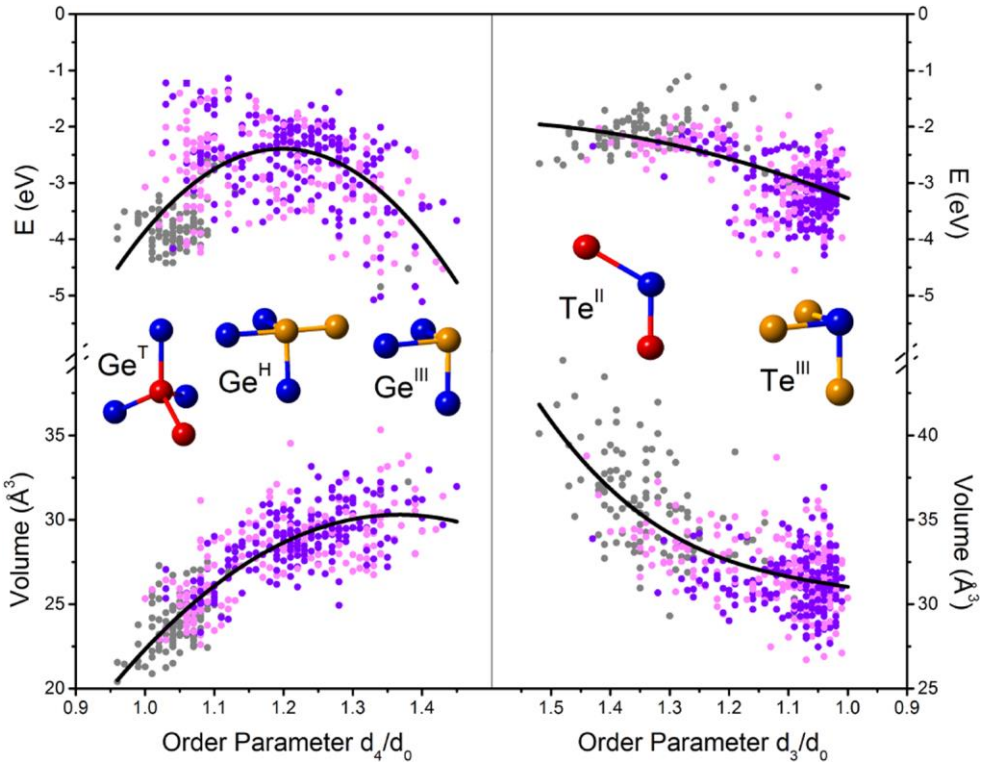

Figure 5. Local energy and local volume for different Ge and Te local geometries in GeTe model structures obtained by MQ and by chemical substitution in SiTe, GeSe and SnTe amorphous structures (corresponding to different symbol colors). The energies and volumes for Ge (left) and Te (right) are plotted against order parameters. For Ge atoms this order parameter is the ratio between of the 4th shortest atomic distance, d4, and the average of the three shortest distances, d0. For Te, the parameter is the ration of the third distance, d3, to the average of the first two, d0. Representative geometries corresponding to selected order parameter values are shown as insets. Reproduced with permission.[52] Copyright 2015, Springer Nature.

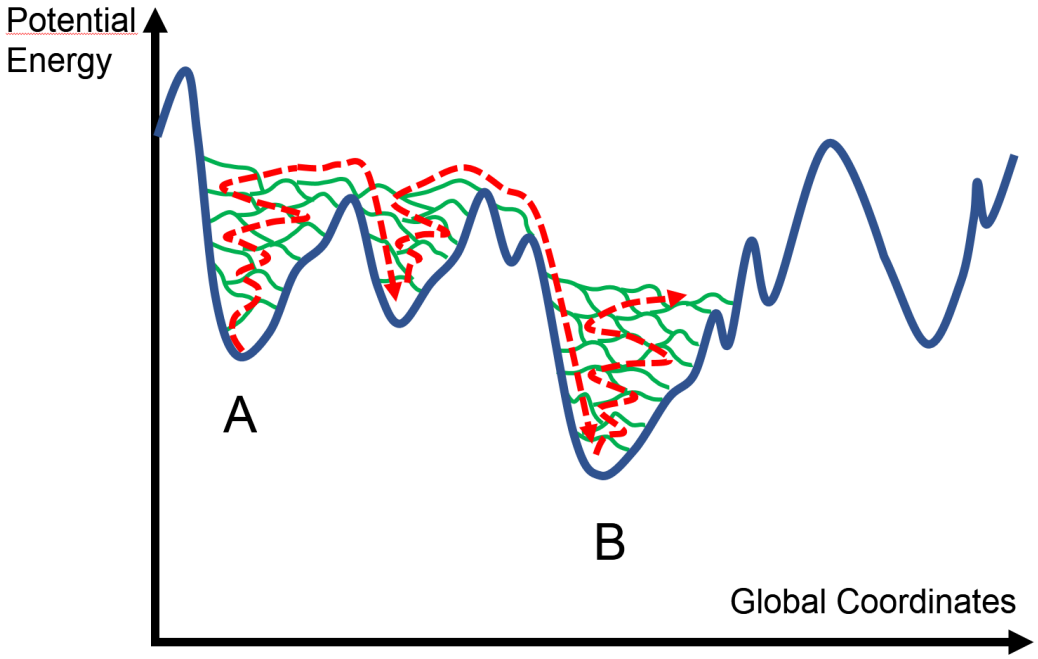

Figure 6. Schematic representation of a metadynamics simulation (the trajectory is represented with red arrows and the potential energy landscape is plotted in blue). Starting from an initial configuration A, an additional potential energy penalty (green lines) is added to each configuration that is sampled along the dynamics trajectory. Therefore, the system progressively escapes from the attraction basin of A and ends up falling into a nearby basin, ultimately reaching the 'ideal' amorphous structure B (the crystal configuration, see Figure 1, is not shown here for simplicity). As penalties constantly add up, the potential energy landscape can be fully reconstructed.

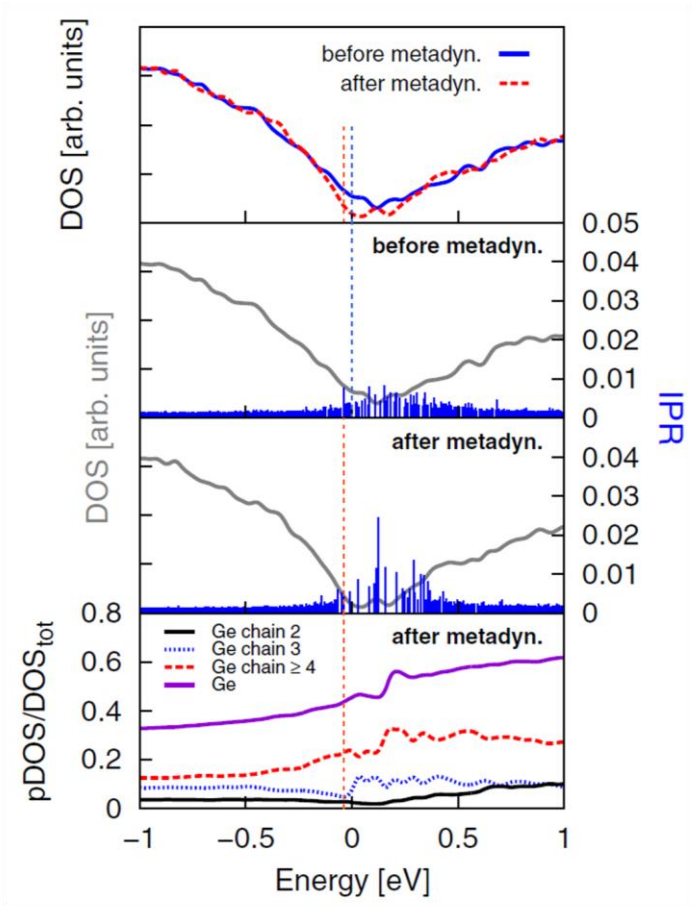

Figure 7. Total density of states (top panel) and corresponding normalized contribution of various Ge local environments (bottom panel) and inverse participation ratio (middle panels) for amorphous GeTe[56] before and after metadynamics simulation. The metadynamics produces a larger energy gap as band tails and gap states become more localized. The bottom panel shows that these localized states arise mostly from homopolar Ge-Ge bonds especially upon clustering of Ge atoms. Reproduced with permission.[56] Copyright 2015, American Physical Society.

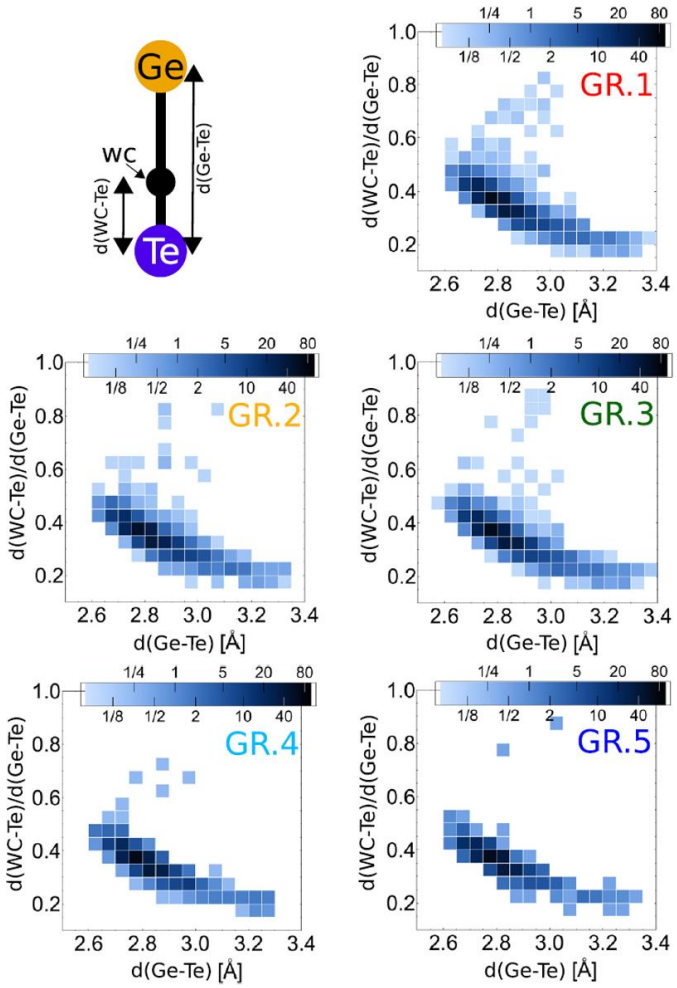

Figure 8. Correlation between the Ge-Te bond length, the 'center' of the bond (measured as the center of a maximally localized Wannier function) and the optical conductivity computed for 44 amorphous GeTe structures. Group 1 to group 5 of structures are defined by their conductivity (from 3000-2500 S/cm for group 1 to 1000-500 S/cm for group 5 using 500S/cm intervals). Two tendencies appear clearly, first, the bond center gets closer to the Te atom as the bond length increases (interpreted as an increase in bond polarization in Ref.[55]), second, the higher conductivity structures have some electrons closer to Ge atoms (attributed in Ref.[55]to over/under coordinated atoms). The color scale indicates the number of bonds in each bin. Reproduced with permission from Ref.[55] Copyright 2016, American Physical Society.

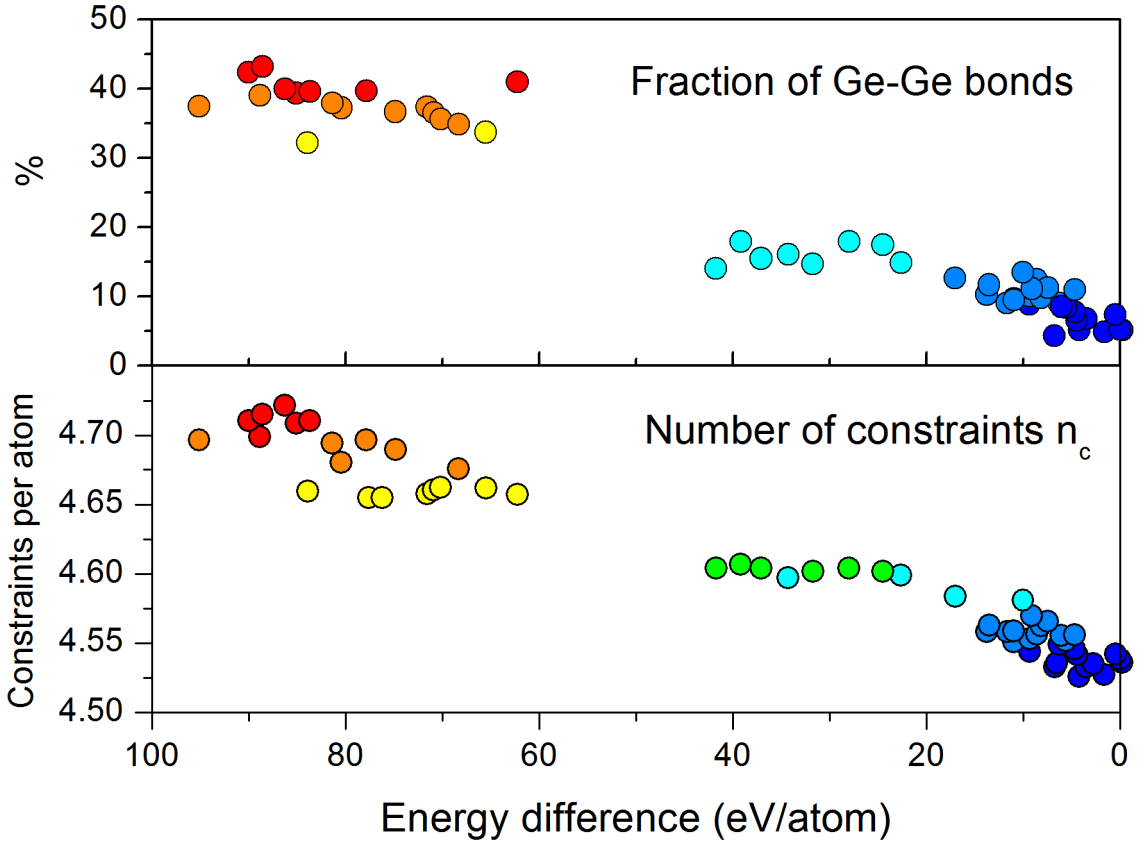

Figure 9. Relation between the fraction of Ge-Ge bonds (top), the number of mechanical constraints per atom (bottom) and the difference in energy between the structure and lowest energy structure found in Ref.[52]. The stabilization of the structure appears to be related to disruption of Ge-Ge bonds and to a number of mechanical constraints that evolves towards that of crystalline GeTe (4.5 constraints per atom). Reproduced with permission.[58] Copyright 2017, Cambridge University Press.

Aging is an important feature of amorphous Phase Change Materials. The various simulation approaches used to improve the description of the glass and to sample their potential energy landscape are reviewed. These methods provide a unique mechanism responsible of aging and the electronic drift, related to the homopolar bonds and tetrahedral Ge motifs.

Keyword

Phase Change Material, Non-volatile Memory, Aging

J.Y. Raty*

Aging in Phase Change Materials : getting Insight from Simulation.

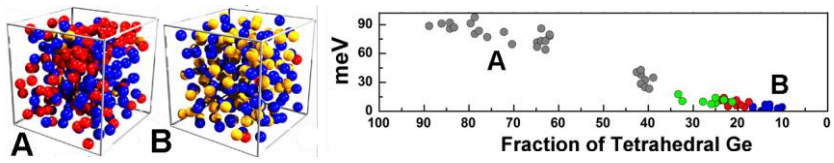

[1] A. Pirovano, A. L. Lacaita, F. Pellizzer, S. A. Kostylev, A. Benvenuti, R. Bez, *IEEE Trans. Electron Devices* **2004**, *51*, 714.
[2] P. Noé, C. Vallée, F. Hippert, F. Fillot, J.-Y. Raty, *Semicond. Sci. Tech.* **2017**, *33*, 013002.
[3] D. Krebs, R. M. Schmidt, J. Klomfaβ, J. Luckas, G. Bruns, C. Schlockermann, M. Salinga, R. Carius, M. Wuttig, *J. Non·Cryst. Solids* **2012**, *358*, 2412.
[4] M. Rütten, M. Kaes, A. Albert, M. Wuttig, M. Salinga, *Sci. Rep.* **2015**, *5*, 17362.
[5] J. Luckas, D. Krebs, S. Grothe, J. Klomfaß, R. Carius, C. Longeaud, M. Wuttig, *J. Mater. Res.* **2013**, *28*, 1139.
[6] M. Boniardi, D. Ielmini, *Appl. Phys. Lett.* **2011**, *98*, 243506.
[7] M. Kaes, M. Salinga, *Sci. Rep.* **2016**, *6*, 31699.
[8] C. A. Angell, K. L. Ngai, G. B. McKenna, P. F. McMillan, S. W. Martin, *J. Appl. Phys.* **2000**, *88*, 3113.
[9] D. Staebler, C. Wronski, *Appl. Phys. Lett.* **1977**, *31*, 292.
[10] E. Johlin, L. K. Wagner, T. Buonassisi, J. C. Grossman, *Phys. Rev. Lett.* **2013**, *110*, 146805.
[11] T. Abtew, M. Zhang, D. Drabold, *Phys. Rev. B* **2007**, *76*, 045212.

[12] K. Vollmayr, W. Kob, K. Binder, *Phys. Rev. B* **1996**, *54,* 15808.
[13] N. Bernstein, J. Feldman, M. Fornari, *Phys. Rev. B* **2006**, *74,* 205202.
[14] L. M. Martinez, C. A. Angell, *Nature* **2001**, *410,* 663.
[15] W. H. Zachariasen, *J. Am. Chem. Soc.* **1932**, *54,* 3841.
[16] J.-Y. Cho, T.-Y. Yang, Y.-J. Park, Y.-C. Joo, *Electrochem. Solid St.* **2012**, *15,* H81.
[17] M. Wimmer, M. Kaes, C. Dellen, M. Salinga, *Frontiers in Physics* **2014**, *2,*
[18] I. V. Karpov, M. Mitra, D. Kau, G. Spadini, Y. A. Kryukov, V. G. Karpov, *J. Appl. Phys.* **2007**, *102,* 124503.
[19] D. Ielmini, M. Boniardi, A. L. Lacaita, A. Redaelli, A. Pirovano, *Microelectronic Engineering* **2009**, *86,* 1942.
[20] J. Luckas, A. Piarristeguy, G. Bruns, P. Jost, S. Grothe, R. M. Schmidt, C. Longeaud, M. Wuttig, *J. Appl. Phys.* **2013**, *113,* 023704.
[21] P. Noé, C. Sabbione, N. Castellani, G. Veux, G. Navarro, V. Sousa, F. Hippert, F. d'Acapito, *J. Phys. D: Appl. Phys.* **2015**, *49,* 035305.
[22] K. Mitrofanov, A. Kolobov, P. Fons, X. Wang, J. Tominaga, Y. Tamenori, T. Uruga, N. Ciocchini, D. Ielmini, *J. Appl. Phys.* **2014**, *115,* 173501.
[23] S. Caravati, M. Bernasconi, T. D. Kühne, M. Krack, M. Parrinello, *Appl. Phys. Lett.* **2007**, *91,* 171906.
[24] W. Wełnic, S. Botti, L. Reining, M. Wuttig, *Phys. Rev. Lett.* **2007**, *98,* 236403.
[25] J. Akola, R. O. Jones, *Phys. Rev. Lett.* **2008**, *100,* 205502.
[26] J. Akola, R. O. Jones, S. Kohara, S. Kimura, K. Kobayashi, M. Takata, T. Matsunaga, R. Kojima, N. Yamada, *Phys. Rev. B* **2009**, *80,* 020201.
[27] J. Hegedus, S. Elliott, *Phys. Status Solidi A* **2010**, *207,* 510.
[28] J.-Y. Raty, C. Otjacques, J.-P. Gaspard, C. Bichara, *Solid State Sci.* **2010**, *12,* 193.
[29] M. Micoulaut, J.-Y. Raty, C. Otjacques, C. Bichara, *Phys. Rev. B* **2010**, *81,* 174206.
[30] R. Mazzarello, S. Caravati, S. Angioletti-Uberti, M. Bernasconi, M. Parrinello, *Phys. Rev. Lett.* **2010**, *104,* 085503.
[31] B. Huang, J. Robertson, *Phys. Rev. B* **2010**, *81,* 081204.
[32] J. Akola, J. Larrucea, R. Jones, *Phys. Rev. B* **2011**, *83,* 094113.
[33] G. Ghezzi, J.-Y. Raty, S. Maitrejean, A. Roule, E. Elkaim, F. Hippert, *Appl. Phys. Lett.* **2011**, *99,* 151906.
[34] J. Kalikka, J. Akola, J. Larrucea, R. Jones, *Phys. Rev. B* **2012**, *86,* 144113.
[35] D. Loke, T. Lee, W. Wang, L. Shi, R. Zhao, Y. Yeo, T. Chong, S. Elliott, *Science* **2012**, *336,* 1566.
[36] G. C. Sosso, J. Behler, M. Bernasconi, *Phys. Status Solidi B* **2012**, *249,* 1880.
[37] S. J. Park, M. H. Jang, S. J. Park, M. Ahn, D. B. Park, D.-H. Ko, M.-H. Cho, *J. Mater. Chem.* **2012**, *22,* 16527.
[38] J.-Y. Raty, P. Noé, G. Ghezzi, S. Maîtrejean, C. Bichara, F. Hippert, *Phys. Rev. B* **2013**, *88,* 014203.
[39] B. Prasai, M. E. Kordesch, D. A. Drabold, G. Chen, *Phys. Status Solidi B* **2013**, *250,* 1785.
[40] W. Zhang, I. Ronneberger, P. Zalden, M. Xu, M. Salinga, M. Wuttig, R. Mazzarello, *Sci. Rep.* **2014**, *4,* 6529.
[41] V. L. Deringer, W. Zhang, M. Lumeij, S. Maintz, M. Wuttig, R. Mazzarello, R. Dronskowski, *Angew. Chem. Int. Edit.* **2014**, *53,* 10817.
[42] S. Caravati, M. Bernasconi, *Phys. Status Solidi B* **2015**, *252,* 260.
[43] J.-Y. Raty, C. Otjacques, R. Peköz, V. Lordi, C. Bichara, in *Molecular Dynamics Simulations of Disordered Materials: From Network Glasses to Phase-Change Memory Alloys* (Eds: C. Massobrio, J. Du, M. Bernasconi and P. S. Salmon), Springer, Cham, Switzerland, **2015**, pp. 485-509.
[44] M. Micoulaut, A. Piarristeguy, H. Flores-Ruiz, A. Pradel, *Phys. Rev. B* **2017**, *96,* 184204.

[45] H. Weber, M. Schumacher, P. Jóvári, Y. Tsuchiya, W. Skrotzki, R. Mazzarello, I. Kaban, *Phys. Rev. B* **2017**, *96*, 054204.
[46] A. Bouzid, G. Ori, M. Boero, E. Lampin, C. Massobrio, *Phys. Rev. B* **2017**, *96*, 224204.
[47] A. Bouzid, C. Massobrio, M. Boero, G. Ori, K. Sykina, E. Furet, *Phys. Rev. B* **2015**, *92*, 134208.
[48] G. C. Sosso, G. Miceli, S. Caravati, J. Behler, M. Bernasconi, *Phys. Rev. B* **2012**, *85*, 174103.
[49] F. C. Mocanu, K. Konstantinou, T. H. Lee, N. Bernstein, V. L. Deringer, G. Csányi, S. R. Elliott, *J. Phys. Chem. B* **2018**,
[50] C. Qiao, Y. Guo, F. Dong, J. Wang, H. Shen, S. Wang, M. Xu, X. Miao, Y. Zheng, R. Zhang, *J. Mater. Chem. C* **2018**, *6*, 5001.
[51] J. Kalikka, J. Akola, R. O. Jones, *Phys. Rev. B* **2014**, *90*, 184109.
[52] J. Y. Raty, W. Zhang, J. Luckas, C. Chen, R. Mazzarello, C. Bichara, M. Wuttig, *Nat. Commun.* **2015**, *6*, 7467.
[53] the semi-empirical nature of the Grimme D2 functional is arguable as the functional dependency on the local atomic environment is fixed and the internal polarizabilty coefficients are not adjusted to experimental values but to ab initio computed reference values instead.
[54] S. Gabardi, E. Baldi, E. Bosoni, D. Campi, S. Caravati, G. Sosso, J. Behler, M. Bernasconi, *J. Phys. Chem C* **2017**, *121*, 23827.
[55] F. Zipoli, D. Krebs, A. Curioni, *Phys. Rev. B* **2016**, *93*, 115201.
[56] S. Gabardi, S. Caravati, G. Sosso, J. Behler, M. Bernasconi, *Phys. Rev. B* **2015**, *92*, 054201.
[57] J. Gaspard, F. Marinelli, A. Pellegatti, *EPL* **1987**, *3*, 1095.
[58] A. Piarristeguy, A. Pradel, J.-Y. Raty, *MRS Bulletin* **2017**, *42*, 45.
[59] H. M. Flores-Ruiz, G. G. Naumis, *Phys. Rev. B* **2011**, *83*, 184204.
[60] H. M. Flores-Ruiz, G. G. Naumis, *J. Chem. Phys.* **2009**, *131*, 154501.